Ink-dependent *n*-factors for the Yule-Nielsen modified spectral Neugebauer model

Romain Rossier, Roger D. Hersch, School of Computer and Communication Sciences, Ecole Polytechnique Fédérale de Lausanne (EPFL), Switzerland

Abstract

Different inks may have different mechanical and/or optical properties. Existing Yule-Nielsen modified Neugebauer spectral prediction models assume however that the inks forming a color halftone behave similarly, i.e. that a single n-factor can model the lateral propagation of light within the paper as well as non-uniformities of the ink dot thickness profiles. However, if the inks have very different optical or mechanical properties, each ink may be separately modeled with its specific n-factor. In order to predict the reflection spectrum of such color halftones, we extend the ink spreading enhanced Yule-Nielsen modified spectral Neugebauer (EYNSN) model by calculating for each halftone an optimal n-factor as an average of the ink specific n-factors weighted by a parabolic function of the ink surface coverages. We compare the prediction accuracies of the standard EYNSN model where each halftone is predicted by making use of one global n-factor with the predictions accuracies of the extended EYNSN model where each halftone is predicted with its corresponding optimal n-factor derived from the individual ink-specific n-factors. For inks having very different optical and/or mechanical properties, we observe an improvement of the prediction accuracies.

Introduction

Many different phenomena influence the reflection spectrum of a color halftone patch printed on a diffusely reflecting substrate (e.g. paper). These phenomena comprise the surface (Fresnel) reflection at the interface between the air and the print, light scattering and reflection within the substrate (i.e. the paper bulk), and the internal (Fresnel) reflections at the interface between the print and the air. The lateral scattering of light within the paper substrate and the internal reflections at the interface between the print and the air are responsible for what is generally called optical dot gain, also known as the Yule-Nielsen effect.

Due to the printing process, the deposited ink dot surface coverage is generally larger than the nominal surface coverage, yielding a "mechanical" dot gain responsible for the ink spreading phenomenon [1]. Effective ink dot surface coverages depend on the inks, on the paper, and also on the specific superposition of an ink halftone and other inks. At the present time, according to the literature [1], [2], [3], among the existing spectral reflection prediction models, mainly the well-known Yule-Nielsen modified spectral Neugebauer model (YNSN) [5], [6] is used for predicting reflection spectra. This model is further enhanced by accounting for the ink spreading phenomenon (denomination: EYNSN) [4]. Ink spreading accounts for the respective mechanical dot gains of each ink halftone printed in the different superposition conditions, i.e. alone on paper, in superposition with one ink, in superposition with two inks and in superposition with three inks. Effective dot surface coverages are fitted separately for every superposition condition by minimizing a difference metric between measured reflection spectrum and predicted reflection spectrum. This yield for each ink halftone and each superposition condition an ink spreading curve mapping nominal to effective surface coverages [4]. To predict the spectral reflectance of a color halftone, nominal surface coverage values are converted into effective coverage values by weighting the contributions of the different ink spreading curves according to the ratios of colorant surface coverages.

In the EYNSN model [4], the effective surface coverages are computed by assuming that the Yule-Nielsen *n*-factor representative of the optical dot gain is the same for all inks. However, as being shown by Hebert and Hersch [7], the Yule-Nielsen *n*-factor also accounts for the non-uniformity of the ink dot thickness profile. Therefore, the Yule-Nielsen *n*-factor may be different for each ink. In addition, some inks are more diffusing than other inks. Hence, the light diffusing property of an ink may therefore also influence the optimal *n*-factor. We observed that the EYNSN model does not predict well reflection spectra of color halftones printed with a combination of inks that behave differently, i.e. a combination of diffusing inks and non diffusing inks or of daylight fluorescent inks and classical inks.

In the present contribution, we extend the EYNSN model by introducing one best *n*-factor per ink. We find by computation the best *n*-factor of each individual ink by minimizing a difference metric between predicted and measured spectral reflectances. In order to adapt the optimal ink spreading curves to all possible values of the *n*-factors, we create a function expressing the fitted optimal ink dot gain at 50% nominal surface coverage as a function of the *n*-factor. The optimal *n*-factor of a color halftone patch is computed by weighting the inks best *n*-factors according to a parabolic function of their nominal surface coverages. The optimal *n*-factor for given nominal surface coverages then defines the optimal ink spreading curves.

The proposed approach takes into account the specific properties of each ink. A test was carried out by printing with ink-jet halftones composed of daylight fluorescent inks and normal inks. For that test, we obtained an improvement of the reflectance prediction accuracies. A second test was performed with normal toner halftones on a laser printer. In this last test, prediction accuracies were only slightly improved. The model extension we propose offers flexibility for cases where the optical or mechanical properties of the inks are very different. The model extension always improves accuracies, even if the improvement is very small for classical inks.

Ink spreading curves enhanced Yule-Nielsen modified spectral Neugebauer model (EYNSN)

The ink spreading model accounting for ink spreading in all ink superposition conditions [4] relies on ink

spreading curves mapping nominal surface coverages to effective surface coverages for (a) the surface coverages of single ink halftones, (b) the surface coverages of single ink halftones superposed with one solid ink and (c) the surface coverages of single ink halftones superposed with two solid inks. In order to obtain the effective coverages (c', m', y') of a color halftone as a function of its nominal surface coverages (c, m, y), the contributions of the different ink spreading curves are weighted according to the ratios of colorants forming that halftone.

During calibration of the model, the ink spreading curves of single ink halftones printed in superposition with paper white, with one solid ink or with two solid inks are obtained by measuring the reflection spectra $R(\lambda)$ at 25%, 50% and 75% nominal surface coverages and by fitting effective surface coverages using the Yule-Nielsen modified spectral Neugebauer model (YNSN) [6]

$$R(\lambda) = \left(\sum_i a_i \, R_i(\lambda)^{1/n} \right)^n \tag{1}$$

where a_i is the surface coverage, $R_i(\lambda)$ is the reflection spectrum of i^{th} *colorant* (also called Neugebauer primary) and n is the Yule-Nielsen factor accounting for the lateral propagation of the light, for variations of ink dot thicknesses and possibly for the diffusing behaviors of the inks ($1< n <100$).

We obtain the ink spreading curves mapping nominal to effective surface coverages for each ink, in each ink superposition condition, by linear interpolation between the fitted effective surface coverages.

For cyan, magenta and yellow inks with nominal coverages c, m and y, the ink spreading functions (curves) mapping nominal coverages to effective coverages for single ink halftones are $f_c(c)$, $f_m(m)$ and $f_y(y)$. The functions mapping nominal coverages of an ink to effective coverages of that ink, for single ink halftones superposed with a second solid ink and for single ink halftones superposed with two solid inks are respectively $f_{c/m}(c)$, $f_{c/y}(c)$, $f_{m/c}(m)$, $f_{m/y}(m)$, $f_{y/c}(y)$, $f_{y/m}(y)$ and $f_{c/my}(c)$, $f_{m/cy}(m)$, $f_{y/cm}(y)$, where $f_{i/j}(i)$ indicates an ink halftone i superposed with solid ink j, and where $f_{i/jk}(i)$ indicates an ink halftone i superposed with solid inks j and k. In the case of three inks, these 12 ink spreading functions may for example be obtained by fitting 36 patches, i.e. 3 patches (25%, 50% and 75% nominal surface coverages) per function. The ink spreading functions may also be obtained by fitting only the effective surface coverage at 50% nominal surface coverage. Effective surface coverages are fitted by minimizing the sum of square differences between predicted reflectance and measured reflectance.

There is one dot gain curve per ink spreading function. The mechanical dot gain is defined as the difference between effective and nominal surface coverage on an ink halftone i in a given superposition condition, i.e $g_i(i) = f_i(i)–i$, $g_{i/j}(i) = f_{i/j}(i)–i$ and $g_{i/jk}(i) = f_{i/jk}(i)–i$. Hereinafter, the term "dot gain" refers to the mechanical dot gain.

In order to obtain the effective surface coverages c', m' and y' of a color halftone patch, it is necessary, for each ink, to weight the contributions of the corresponding ink spreading curves. For example, for deducing the effective cyan ink halftone surface coverage, we need to weight the contributions of the ink spreading curves f_c, $f_{c/m}$, $f_{c/y}$ and $f_{c/my}$. The weighting functions depend on the effective surface coverages of the colorants on which the considered ink halftone is superposed. Let us assume that inks are printed independently of each other. For the considered system of 3 inks *cyan*, *magenta* and *yellow* with nominal coverages c, m and y and effective coverages c', m' and y', the equations (2) weight each ink spreading curve with the corresponding relative surface of its underlying colorants.

In analogy with Demichel's equations (3), the relative weight of the underlying white colorant (*cyan* superposed with colorant paper white only) is $(1-m')(1-y')$, the relative weight of the underlying magenta colorant (*cyan* superposed with colorant *magenta* only) is $m'(1-y')$, the relative weight of the underlying yellow colorant (*cyan* superposed with colorant *yellow* only) is $(1-m')y'$ and the relative weight of the underlying red colorant (*cyan* superposed with both solid *magenta* and *yellow*) is $m'y'$. The resulting system of equations is [4]:

$$\begin{aligned}
c' = {} & f_c(c)(1-m')(1-y') + f_{c/m}(c)m'(1-y') \\
& + f_{c/y}(c)(1-m')y' + f_{c/my}(c)m'y' \\
m' = {} & f_m(m)(1-c')(1-y') + f_{m/c}(m)c'(1-y') \\
& + f_{m/y}(m)(1-c')y' + f_{m/cy}(m)c'y' \\
y' = {} & f_y(y)(1-c')(1-m') + f_{y/c}(y)c'(1-m') \\
& + f_{y/m}(y)(1-c')m' + f_{y/cm}(y)c'm'
\end{aligned} \tag{2}$$

This system of equations can be solved iteratively: one starts by setting initial values of c', m' and y' equal to the respective nominal coverages c, m and y. After one iteration, one obtains new values for c', m' and y'. These new values are used for the next iteration. After a few iterations, typically 4 to 5 iterations, the system stabilizes and the obtained coverages c', m' and y' are the effective coverages. The system of equations (2) yields the effective surface coverages of cyan, magenta and yellow inks for the corresponding nominal surface coverages.

The effective colorant surface coverages of Neugebauer primaries are obtained from the effective coverages of the inks according to the Demichel equations (3) which give the respective surface coverages of the colorants as a function of the surface coverages of the individual inks. In case of independently printed cyan, magenta and yellow inks of respective surface coverages c', m', y', the respective fractional areas of the colorants white, cyan, magenta, yellow, red (superposition of *magenta* and *yellow*), green (superposition of *yellow* and *cyan*), blue (superposition of *magenta* and *cyan*) and black (superposition of *cyan*, *magenta* and *yellow*) are :

White	$a'_w = (1-c')(1-m')(1-y')$
Cyan	$a'_c = c'(1-m')(1-y')$
Magenta	$a'_m = (1-c')m'(1-y')$
Yellow	$a'_y = (1-c')(1-m')y'$
Red	$a'_r = (1-c')m'y'$
Green	$a'_g = c'(1-m')y'$
Blue	$a'_b = c'm'(1-y')$
Black	$a'_k = c'm'y'$

(3)

The complete model accounting for ink spreading in all superposition conditions is illustrated in Figure 1. The n-factor of the Yule-Nielsen modified spectral Neugebauer

model for a given printer and screen element frequency is obtained by computing for a subset of the considered color samples the mean CIELAB ΔE_{94} color difference between predicted and measured reflection spectra. By iterating across possible *n*-factors, one selects the *n*-factor yielding the lowest mean color difference between predicted and measured reflection spectra.

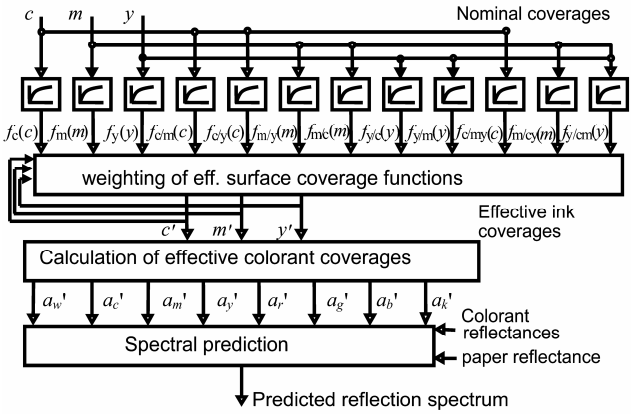

Figure 1. *Prediction model with ink spreading in all superposition conditions.*

Extending the EYNSN spectral prediction model with ink dependent *n*-factors

In the following experiment, we illustrate the impact of varying for each ink the Yule-Nielsen *n*-factor. In Figure 2, we plot the prediction error (ΔE_{94}) as function of the dot gain, for different *n*-factors. We consider separately the standard cyan ink, the daylight fluorescent magenta ink (abbreviated magenta fluo) and the daylight fluorescent yellow ink (abbreviated yellow fluo). The three curves of Figure 2 show the prediction error for *n*-factors of 1, 6 and 14. On each curve, the circle represents the smallest achievable prediction error for a given *n*-factor and its corresponding dot gain.

The best achievable *n*-factors for the cyan, the magenta fluo and the yellow fluo inks are respectively 14, 2 and 1. In the classical EYNSN [4] model we choose the *n*-factor that minimizes the sum of square differences between predicted and measured reflectance spectra in all ink superposition conditions. For the present set of cyan, magenta fluo and yellow fluo, the overall optimal single *n*-factor provided by the EYNSN model is 6 which introduces a cyan prediction error of ΔE_{94}=0.9 (Figure 2a, circle on dotted line) and a yellow fluo prediction error of ΔE_{94}=1.37 (Figure 2c, circle on dotted line). However, if we take the best *n*-factor for the cyan and the yellow fluo inks, the prediction errors decrease from ΔE_{94}=0.9 to ΔE_{94}=0.54 (Figure 2a, double circle) and from ΔE_{94}=1.37 to ΔE_{94}=0.46 (Figure 2c, double circle). Therefore, for this combination of inks, the choice of the *n*-factor has a strong impact on the spectral prediction accuracy. We observed that the best *n*-factor of one ink in the different superposition conditions remains the same. For instance, when we fit the best *n*-factor for the yellow fluo on paper only, on solid magenta fluo, on solid cyan and on solid magenta fluo and cyan, the best *n*-factor remains 1. We observed similar results for the cyan and the magenta fluo in the different superposition conditions.

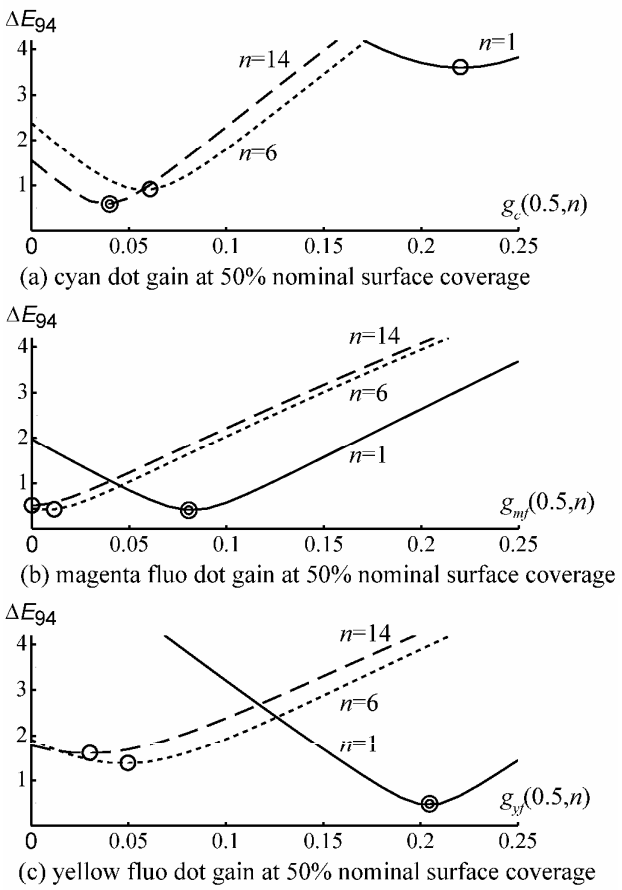

Figure 2. *Color difference ΔE_{94} as a function of n-factor and mechanical dot gain for (a) cyan on paper, (b) magenta fluo on paper and (c) yellow fluo on paper. The circles show the best dot gain for a given n-factor. Double circles show the optimal combination of n-factor and mechanical dot gain.*

From the experiments performed above, we conclude that there is a need of taking into account the best *n*-factor of each individual ink. We therefore extend the EYNSN model so as to be able to predict the reflection spectrum of color patches by using the best *n*-factor for each ink. At model calibration, we construct in each superposition condition one curve establishing the relationship between *n*-factor and optimal mechanical dot gain. Figure 3a illustrates the optimal mechanical dot gain *g* in function of the *n*-factor for the cyan on paper ink superposition at 25%, 50% and 75% nominal surface coverages. When predicting the reflectance of a halftone of given surface coverages, we select the optimal overall *n*-factor by weighting the best *n*-factors of the individual inks according to a function of their ink surface coverages. For a system of 3 inks with nominal surface coverages c_1, c_2, c_3 and corresponding best *n*-factors n_1, n_2 and n_3 fitted as 50% nominal surface coverages, we calculate the n_{opt}-factor

$$n_{\text{opt}} = \begin{cases} \dfrac{n_1 \cdot p(c_1) + n_2 \cdot p(c_2) + n_3 \cdot p(c_3)}{p(c_1) + p(c_2) + p(c_3)} & \text{if } c_1 + c_2 + c_3 \neq 0 \\ 1 & \text{otherwise} \end{cases} \quad (4)$$

where $p(c)$ is the parabola equation

$$p(c) = -4 \cdot (c - 1/2)^2 + 1 \quad (5)$$

The *n*-factor does not influence the spectral prediction of solid colorants. The *n*-factor having a maximal impact is the one of a halftone at 50% nominal surface coverage. The parabolic function of the surface coverage (5) is continuous, yields a maximum at a surface coverage of 0.5 and zero values at surface coverages of 0 and 1. It is therefore well adapted for weighting the *n*-factors.

With the optimal *n*-factor calculated according to Eqs. (4) and (5) for a given halftone, we select from the previously established dot gain curves as a function of *n*-factor the dot gains $g_i(i,n_{opt})$ at i=0.25, i=0.5 and i=0.75 nominal surface coverages. Then, by linear interpolation, we obtain the dot gain curve g_i. The other dot gain curves $g_{i/j}$, $g_{i/jk}$ are obtained in the same manner. Figure 3 illustrates how to obtain the dot gain curve of the cyan on paper ink superposition condition at an *n*-factor of 3.

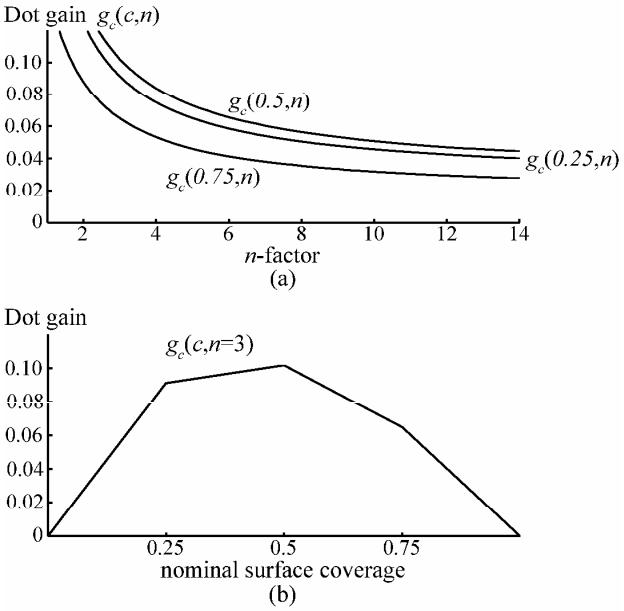

Figure 3. *(a) Mechanical dot gain for cyan printed on paper at 25%, 50% and 75% nominal surface coverages for all n-factors between 1 and 14 and (b) corresponding dot gain curve for an n-factor n_{opt}=3.*

The ink spreading curves $f_i(i)$, $f_{i/j}(i)$ and $f_{i/jk}(i)$ are calculated by adding the nominal surface coverages to the dot gain, i.e. $f_i(i) = g_i(i) + i$, $f_{i/j}(i) = g_{i/j}(i) + i$ and $f_{i/jk}(i) = g_{i/jk}(i) + i$. The next steps are the same as with the single *n*-factor EYNSN model, i.e. we compute effective ink surface coverages according to Eq. (2), effective colorant surface coverages according to Eq. (3) and calculate the predicted reflection spectrum according to Eq (1), with $n = n_{opt}$. Note that in the proposed variable *n*-factor EYNSN model, for each predicted color halftone, one optimal *n*-factor is calculated and therefore one set of new ink spreading curves is generated.

Since at model calibration we construct for each ink superposition condition one curve establishing the relationship between *n*-factor and mechanical dot gain, we need to fit the dot gains $g(i,n)$ for 12 ink superposition conditions. Usually, we consider the *n*-factors by step of 0.2 between 1 and 14 (66 *n*-factors) and nominal coverages at i=0.25, i=0.5 and i=0.75, yielding 2178 fitted dot gain values. The sum of square differences between predicted and measured spectral reflectance metric minimization is carried out with a computer executable procedure implementing Powell's function minimization [8] and takes approximatively 0.015s within a matlab framework running on an Athlon 64X2 5000+ processor at 2.6 GHz. Therefore, the total calibration time does not exceed 39s which is reasonable since only one calibration is performed for a combination of printer, inks and halftoning algorithm. Once all calibrated values have been stored in a lookup table, the overhead introduced by the ink-dependent *n*-factor model compared with the EYNSN model consists in computing the optimal *n*-factor according to Eq. (4). While spectral predictions take in average 83ms with the EYNSN model, the same spectral predictions take in average 92ms with the ink dependent *n*-factor model. These timing figures rely on code written in Matlab using general purpose library functions. The processing times could be seriously improved by making use of an efficient programming language such as C/C++ or Java.

Results

We preformed spectral predictions with both the EYNSN model and the variable *n*-factor EYNSN model. In addition, we performed spectral predictions with an ideal variable optical dot gain spectral prediction model where each test sample is predicted by using an individually fitted *n*-factor yielding the best prediction accuracy. The experiments were performed on an ink jet printer (Canon Pixma Pro 9500 at 600 dpi) with cyan, daylight fluorescent magenta and daylight fluorescent yellow inks and on a laser printer (Brother HL-4000) with standard cyan, magenta and yellow toners. The test samples are printed on Canon MP-101 paper at a screen frequency of 120lpi, at all combinations of nominal ink surface coverages 0, 0.25, 0.5, 0.75 and 1 (5^3 = 125 test patches). Table 1 gives the mean reflectance prediction error in terms of ΔE_{94} values, the maximal prediction error, the 95% quantile prediction error and the reflectance mean sum of square differences (ssd) prediction error. Reflectances were measured with a DataColor MF45 spectro-photometer with the geometry (45°d:0°), i.e. 45° incident directed beam and zero degree capture. For calculating the ink spreading curves, 25%, 50% and 75% nominal coverages in each superposition conditions are considered: either for one single *n*-factor in the EYNSN model or for all *n*-factors by steps of 0.2 between 1 and 14 for the variable *n*-factor EYNSN model.

The spectral prediction based on a variable ink-dependent *n*-factor for the EYNSN model is more accurate than the stand-alone EYNSN model. When mixing daylight fluorescent inks with normal inks, the ΔE_{94} mean prediction error decreases from 1.25 to 1.08 (Table 1). This is due to the completely different optical properties of the cyan ink and the yellow fluo ink (Figs. 2a and 2c). For these two inks, we observe a large difference in accuracy between the minima at different *n*-factors. The best minimum is either at a low *n*-factor (n=1) for the yellow fluo ink or at a very high *n*-factor (n=14) for the cyan ink. Therefore, a single *n*-factor cannot provide a high prediction accuracy.

In the case of classical electrophotographic printing with standard toners, we observe only slightly improved prediction accuracies. Even if the best *n*-factors for the yellow and the cyan toners are different (see Table 3), the prediction accuracies at different *n*-factors are close to each other. Therefore, predicting reflection spectra with the halftone dependent optimal *n*-factors decreases the mean

ΔE_{94} only from 1.26 to 1.23 and the 95% quantile from 3.13 to 3.05.

The comparison between the ideal model and the variable ink-dependent *n*-factor EYNSN model shows that the optimal *n*-factor calculated with the ink specific *n*-factors according to Eqs. (4) and (5) is close to *n*-factors individually fitted to each patch. Within the present framework having one optimal *n*-factor for each patch provides the highest possible prediction accuracy and represents therefore a "ground truth", adapted to the considered combination of printer, paper and inks. For the Canon Pro 9500 test set, the mean ΔE_{94} accuracy difference between the ground truth and the ink-dependent *n*-factor model is 0.02 and for the Brother 4000-HL test set, this mean accuracy difference is only 0.04.

Finally, the results illustrate the improved flexibility offered by the variable *n*-factor EYNSN spectral prediction model which accounts for the different optical properties of the inks. Inks with different properties show improved prediction accuracies and inks with similar properties show either no improvement or a small improvement in prediction accuracies.

Table 1. Prediction accuracies for cyan, magenta fluo and yellow fluo test samples printed with a Canon pro 9500 inkjet printer and for cyan, mangenta, yellow test samples printed with a Brother 4000-HL laser printer.

Test sets	ΔE_{94}			*ssd*
Model EYNSN	avg	95%	max	avg
Canon Pro 9500				
Single n-factor	1.25	3.3	2.73	0.00642
Ink dependent n-factor	1.08	3.3	2.69	0.00562
Ideal	1.06	3.3	2.63	0.00542
Brother 4000-HL				
Single n-factor	1.26	5.20	3.13	0.00177
Ink dependent n-factor	1.23	5.13	3.05	0.00175
Ideal	1.19	5.10	3.10	0.00166

Table 2. Canon pro 9500 ΔE_{94} prediction accuracies for the cyan, magenta fluo and yellow fluo best *n*-factors.

ΔE_{94} at	n_c=14	n_{mf}=2	n_{yf}=1
Cyan	0.54	2.00	3.60
Magenta fluo	0.50	0.14	0.41
Yellow fluo	1.60	0.60	0.46

Table 3. Brother 4000-HL ΔE_{94} prediction accuracies for the cyan, magenta and yellow best *n*-factors.

ΔE_{94} at	n_c=5.6	n_m=11.8	n_y=14
Cyan	0.42	0.78	0.83
Magenta	0.32	0.09	0.11
Yellow	0.46	0.26	0.23

Conclusion

We propose an extension to the ink spreading enhanced Yule-Nielsen spectral Neugebauer model. This extension accounts for the different optical and possibly mechanical properties of the inks. We consider for each ink a specific Yule-Nielsen *n*-factor. Optimal *n*-factors are calculated for halftones composed of several inks by weighting the inks best *n*-factors with a parabolic function of their surface coverages. Compared with the original EYNSN model, prediction accuracies are improved for a set composed of standard and daylight fluorescent inks. They are slightly improved for a set composed of normal toners. The presented approach provides additional flexibility for spectral predictions of halftones produced by inks having significantly different optical or mechanical properties.

Acknowledgement

We thank the Swiss National Science Foundation for their support, grant n° 200020-126757/1.

References

[1] R. Balasubramanian, Optimization of the spectral Neugebauer model for printer characterization, J. Electronic Imaging, Vol. 8, No. 2, 156-166, (1999).

[2] D.R. Wyble, R.S. Berns , A Critical Review of Spectral Models Applied to Binary Color Printing, J. Color Res. Appl., Vol. 25, No. 1, 4-19, (2000).

[3] T. Ogasahara, Verification of the Predicting Model and Characteristics of Dye-Based Ink Jet Printer, Journal of Imaging Science and Technology, Vol. 48, No. 2, 130-137 (2004).

[4] R.D. Hersch, F. Crété, Improving the Yule-Nielsen modified spectral Neugebauer model by dot surface coverages depending on the ink superposition conditions, Color Imaging X: Processing, Hardcopy and Applications, SPIE Vol. 5667 (R. Eschbach, G.G. Marcu eds.), 434-445 (2005).

[5] J.A.C. Yule , W.J. Nielsen, The penetration of light into paper and its effect on halftone reproductions, Proc. TAGA, Vol. 3, 65-76, (1951).

[6] J.A.S Viggiano, Modeling the Color of Multi-Colored Halftones, Proc. TAGA, 44-62, (1990).

[7] M. Hebert, R.D. Hersch, Analyzing halftone dot blurring by extended spectral prediction models, JOSA A, Vol. 27, 6-12 (2010).

[8] W.H. Press, B.P. Flannery, S.A. Teukolsky, W.T. Fetterling, Numerical Recipes, Cambridge University Press, 1st edition, 1988, section 10.5, 309-317.

Author Biography

Romain Rossier *is a PhD student at the Peripheral Systems Laboratory (Ecole Polytechnique Fédérale de Lausanne, or EPFL) in Lausanne, Switzerland. His research interests include color prediction, mathematical modelling of printing processes, color printing with ink-jet methods and security imaging. He graduated a MS in computer science from EPFL in 2007.*

